Identification of SYK inhibitor, R406 as a novel senolytic agent

Hyun-Ji Cho[1,2], Eun Jae Yang[3], Joon Tae Park[4], Jae-Ryong Kim[5], Eok-Cheon Kim[5], Kyong-Jin Jung[5], Sang Chul Park[1,6,7], Young-Sam Lee[1,3]

[1]Well Aging Research Center, DGIST, Daegu 42988, Korea
[2]Department of Medicine, Catholic University of Daegu School of Medicine, Daegu 42472, Korea
[3]Department of New Biology, DGIST, Daegu 42988, Korea
[4]Division of Life Sciences, College of Life Sciences and Bioengineering, Incheon National University, Incheon 22012, Korea
[5]Department of Biochemistry and Molecular Biology, Smart-Aging Convergence Research Center, College of Medicine, Yeungnam University, Daegu 42415, Korea
[6]Department of Molecular Medicine, Chonnam National University Medical School, Gwangju 58128, Korea
[7]The Future Life and Society Research Center, Chonnam National University, Gwangju 58128, Korea

Correspondence to: Hyun-Ji Cho, Young-Sam Lee; **email:** hjcho.dr@gmail.com, lee.youngsam@dgist.ac.kr

ABSTRACT

The selective removal of senescent cells by senolytics is suggested as a potential approach to reverse aging and extend lifespan. Using high-throughput screening with replicative senescence of human diploid fibroblasts (HDFs), we identified a novel senolytic drug R406 that showed selective toxicity in senescent cells. Using flow cytometry and caspase expression analysis, we confirmed that R406 caused apoptotic cell death along with morphological changes in senescent cells. Interestingly, R406 altered the cell survival-related molecular processes including the inhibition of phosphorylation of the focal adhesion kinase (FAK) and p38 mitogen-activated protein kinase (MAPK) in senescent cells. This pattern was not observed in other known senolytic agent ABT263. Correspondingly, apoptotic cell death in senescent cells was induced by simultaneously blocking the FAK and p38 pathways. Taken together, we suggest that R406 acts as a senolytic drug by inducing apoptosis and reducing cell attachment capacity.

INTRODUCTION

Aging is a progressive physiological change over time and is mainly associated with the decline of biological functions and senescence in an organism [1]. The loss of biological function in cells, the basic units of tissue and organ, can be caused by cellular stresses, including genomic instability, impaired proteostasis, and dysfunctional subcellular organelles, all of which provoke the cessation of cell division and cellular senescence [2–5]. Senescent cells have a variety of characteristics such as the irreversible arrest of the cell cycle, resistance to apoptosis, increasing activity of senescence-associated β-galactosidase (SA-β-gal), and secretion of a set of various cytokines involving chronic inflammation and structure remodeling, known as senescence-associated secretory phenotypes (SASPs) [2, 3, 6–9]. Although the transient appearance of cellular senescence plays an essential role in tissue remodeling, efficient immune clearance during embryonic development, and after an injury [10–12], a loss of proliferation capacity and SASP secretion in chronic senescent cells per se affects the repair of impaired tissues. Therefore, cellular senescence is

suggested to be strongly linked with age-associated tissue damage and diseases. Recent evidence also points to close linkage between cellular senescence and tissue dysfunction. Transplanting senescent cells induced physical dysfunction in young mice [13]. In contrast, the clearance of p16[Ink4a]-positive senescent cells extends lifespan in an aging-induced transgenic mouse model, INK-ATTAC mice [14], and a mouse model of a human progeroid syndrome, Ercc1-/ mice [15].

Senotherapeutics, which are small molecules targeting cellular senescence for delaying age-related processes or diseases, have been developed mainly for two uses: one is senomorphic medicines, which suppress cellular senescence and induce reverse senescence phenotypes, and the other is senolytic drugs, which induce cytotoxicity selectively in senescent cells [16]. The combination of dasatinib and quercetin are the first senolytic agents effective in the removal of ionizing radiation-induced senescent cells *in vitro* and alleviating age-related symptoms in the progeroid Ercc1−/Δ mouse model *in vivo* [17]. Emerging evidence has demonstrated that senolytic agents alleviate various age-related conditions in mice, including age-associated vascular phenotypes [18], metabolic dysfunction [19], and osteoarthritis [20], and even affect senescence-related dysfunctions in human [21].

Major classes of senolytic drugs typically focus on inhibiting pro-survival pathways or triggering pro-apoptosis signaling in senescent cells. The combination of dasatinib and quercetin, which reduced p21, PAI-2, and BCL-xL [17], and Navitoclax (ABT263), which targets the Bcl-2 family [22], belong to this class of senolytics. In other classes, the mimicry of forkhead box protein O4 (FOXO4) peptide selectively disrupted the p53-FOXO4 interaction, which induced p53-dependent apoptosis in senescent cells [23]. Recently, a HSP90 inhibitor was identified as a novel class of senolytic drugs that downregulated the phosphorylation of PI3K/AKT, an anti-apoptotic factor [15]. Despite intensified efforts to develop drugs targeting senescent cells, however, the number of senolytic agents is still limited in comparison with the number of drugs against other age-related diseases like cancer or fibrosis. Finding a novel senotherapeutic would expand the spectrum of efficacy on various types and stages of cellular senescence.

In this study, using high-throughput screening (HTS) to measure the variation of cell proliferation and reactive oxygen species (ROS) levels, we identified a novel senolytic agent R406, also known as tamatinib. This agent was effective in the replicative senescence (RS) model of diploid human dermal fibroblasts (HDFs). R406 induced the caspase-9-mediated intrinsic apoptotic pathway, similar to other known senolytic drugs; however, R406 did not significantly change the level of Bcl-2 family in senescent cells. Alternatively, R406 inhibited the phosphorylation of focal adhesion kinase (FAK) as well as p38 mitogen-activated protein kinase (MAPK), which both regulate cell survival. Our results demonstrate that R406 is a new class of senolytics that targets multiple regulatory pathways for senescent cell survival.

RESULTS

R406 reduces cell viability in senescent HDFs

In our previous studies, we evaluated the ability to restore senescent fibroblasts in the RS model using HTS with a library containing 355 kinase inhibitors [24, 25]. From these results, we selected candidates for their senolytic activity based on inducing cytotoxicity, increasing ROS levels, or both (Supplementary Table 1). Next, we selected out second candidate compounds by reviewing the publications on the chosen drugs initially regarding cell physiologies (e.g., senolytic effect, apoptosis, and cell death) and side effects in pre-clinical studies (e.g., high toxicity, diarrhea, fever, rash, etc.). Then, based on the CCK-1 assay, we assessed the differential cytotoxicity of the remaining candidates depending on the state of cellular senescence in HDFs (Supplementary Figure 1). Among these, R406, an FDA-approved Syk inhibitor, was found to exhibit higher cytotoxicity in senescent HDFs than in non-senescent cells over the tested range of concentration (from 1 to 20 μM; Figure 1A). Nintedanib, a tyrosine kinase inhibitor, also showed senolytic effects at lower concentrations (from 1 to 5 μM) but was toxic in higher concentration (20 μM), regardless of the senescent state (Figure 1B). Other drug candidates were not suitable as senolytic drugs due to either non-selective cytotoxicity (NVP-BHG712, an Ephrin type-B receptor 4 inhibitor; AZD, an ALK inhibitor; CCT129202, an aurora kinase inhibitor; and axitinib, a tyrosine kinase inhibitor; Figure 1C–1F); or were drugs that had no cytotoxic effect (bosutinib, an Src inhibitor; and selumetinib, a MEK inhibitor; Supplementary Figure 2A and 2B). In addition, we further confirmed R406-induced cytotoxicity by Hoechst 33342 staining, because CCK-1-based cell viability assay could reflect cell metabolic activity, which might be influenced by kinase inhibitors. Similar to the CCK-1 assay, the fluorescence levels of senescent HDFs were reduced by R406 in a dose dependent manner (Supplementary Figure 2C). Our results demonstrated that R406 has cytotoxicity selectively in senescent fibroblasts in the RS model and, subsequent experiments were performed using R406 concentration of 10 μM.

R406 induces apoptotic cell death

Senescent cells demonstrate elevated expression of anti-apoptotic and pro-survival factors [15, 17, 22]. Typical

senolytic agents inhibit cell viability by modulating expression of these factors, particularly Bcl-2 family [26]. Therefore, we investigated whether the cytotoxic effect of R406 is caused by the induction of apoptosis. R406 induced cell shrinkage in senescent HDFs compared to non-senescent HDFs, and decreased cell number of senescent HDFs. The non-senescent HDFs showed only slightly delayed cell growth with R406 (Figure 2A). Unexpectedly, R406-dependent downregulation of Bcl-2 and Bcl-xl expression was not significant in senescent HDFs as compared to non-senescent HDFs (Figure 2B). Instead, the level of Bim as well as cleaved-caspase-9, -7, and -3 were induced by R406 in senescent HDFs, though the amount of cytochrome C, Bak, Bax, and Bad were also not significantly changed (Figures 2C and 3). The levels of cleaved-caspase-8, an indicator of extrinsic apoptotic signal induction, or cleaved-PARP-1, which is a late apoptotic marker, were not changed by R406 treatment in either senescent or non-senescent cells (Supplementary Figure 3A and Figure 2D, respectively). To confirm that R406 is associated with apoptosis in a senolytic effect, we performed an apoptosis assay by flow cytometry with annexin V and propidium iodide (PI) staining after treating either a vehicle (dimethyl sulfoxide; DMSO) or 10 μM R406 for one day in senescent and non-senescent HDFs. For the analysis, staurosporine was used as a positive control of the apoptotic effect. As a expect, approximately 23% of R406 treated senescent cells were annexin V-positive

compared with only 11% in the R406-treated non-senescent cells. (Figure 2E and 2F). These data indicate that R406 induces apoptotic cell death on senescent cells in the RS model.

Previous studies demonstrated that ABT263 selectively induced apoptotic cell death in ionizing radiation-induced senescent HUVECs, IMR-90 cells, and preadipocytes at the sub-micromolar concentration [22]. Moreover, ABT263 rejuvenated aged hematopoietic stem cells in mice [27]. Thus, we investigated whether R406 can induce an apoptotic effect similar to ABT263. For this purpose, we tested the concentration range at which ABT263 demonstrated a senolytic effect in our system. Contrary to our expectation, a one day exposure of ABT263 (at 0.1~10 μM) was not found to be effective in cytotoxicity in either senescent or non-senescent HDFs (Supplementary Figure 4A–4C) compared with the R406 senolytic effect induced over the same time (Figure 1). Morphological changes and the expression of cleaved-caspase-9, -3 and -7 were induced by ABT263 but only after a three-day exposure at a much higher concentration (more than 1 μM) than conventionally used (Supplementary Figure 4D–4F). Thus, subsequent experiments were performed using 1 μM of ABT263.

In our results, R406 exhibited a senolytic effect one day post-treatment (Figures 1 and 2), whereas most of reported senolytic drugs needed to be treated for two
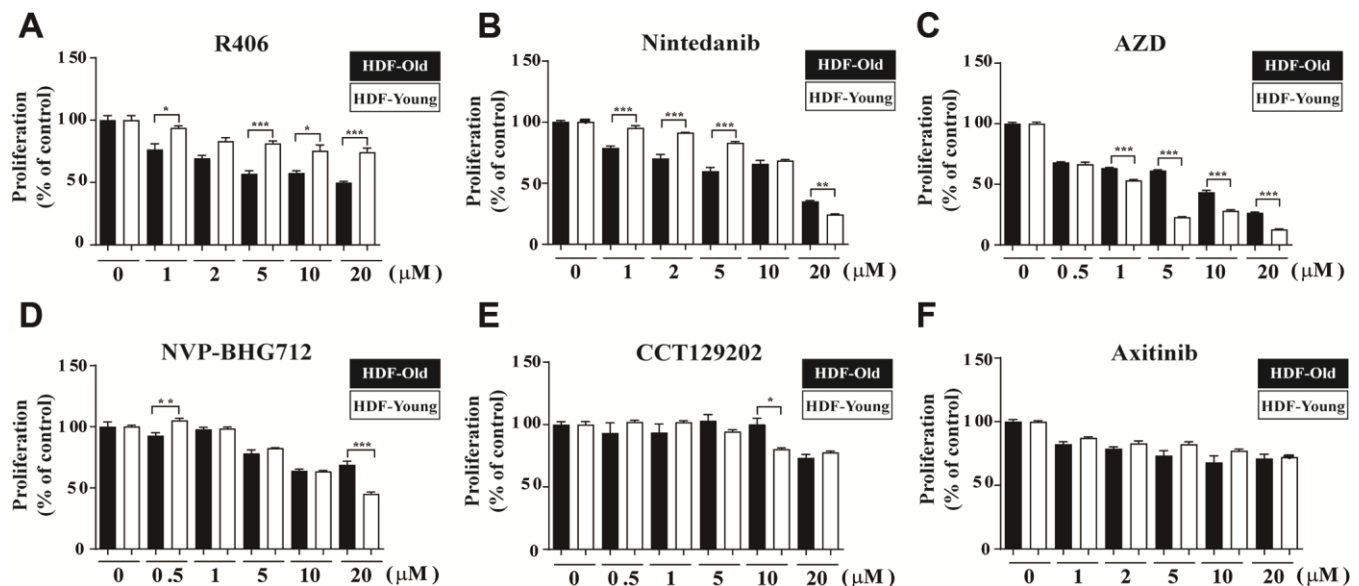
Figure 1. R406 reduces viability of senescent HDFs. Senescent HDFs (HDF-Old) and non-senescent HDFs (HDF-Young) were treated with (**A**) R406 (1, 2, 5, 10, 20 μM), (**B**) Nintedanib (1, 2, 5, 10, 20 μM), (**C**) AZD (0.5, 1, 5, 10, 20 μM), (**D**) NVP-BHG712 (0.5, 1, 5, 10, 20 μM), (**E**) CCT129202 (0.5, 1, 5, 10, 20 μM), and (**F**) Axitinib (1, 2, 5, 10, 20 μM) for one day, and then CCK-1 assays were conducted to investigate cell viability. n = 8, *p<0.05, **p<0.01, ***P<0.001.
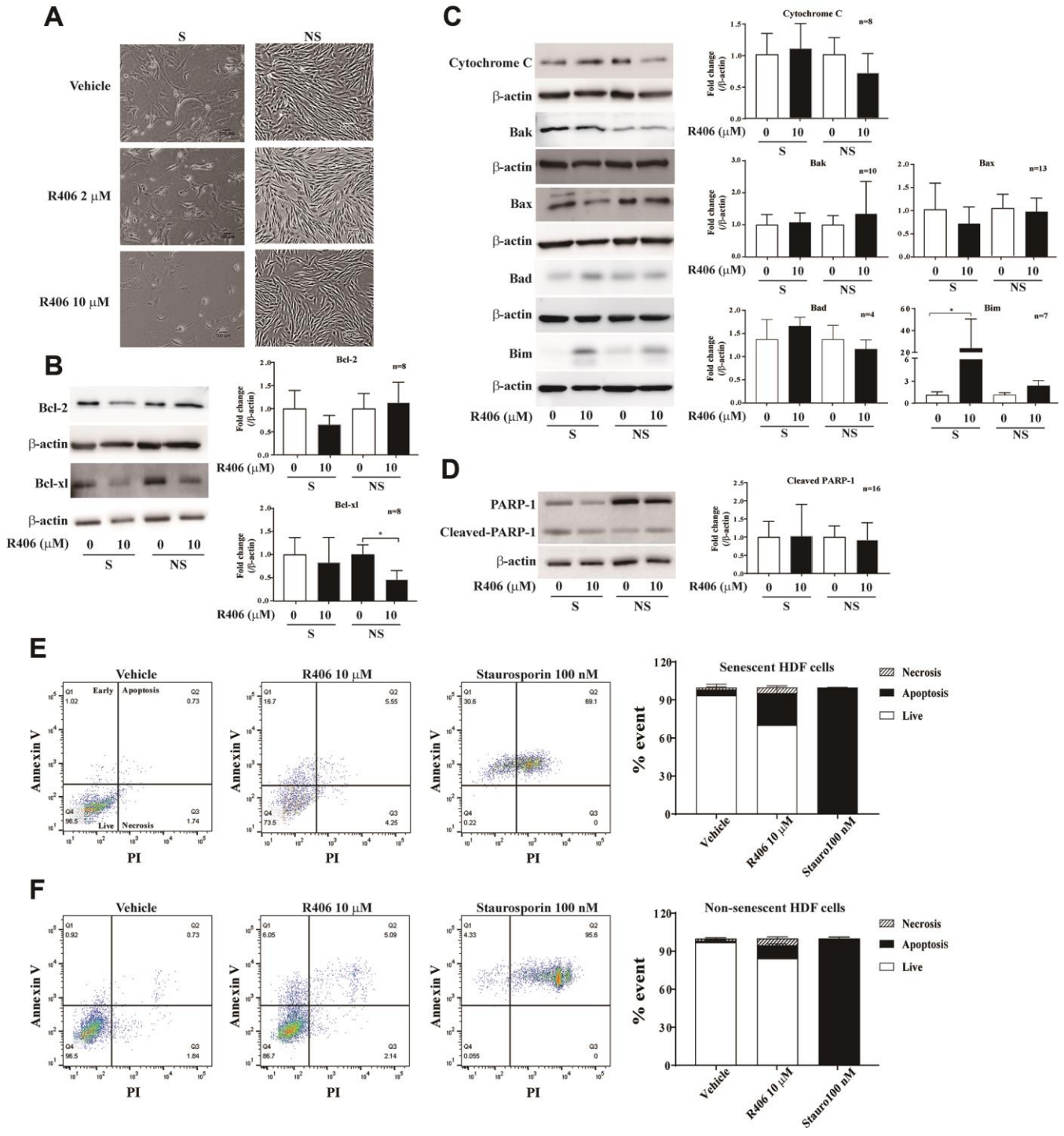
Figure 2. R406 induces apoptotic cell death in senescent HDFs. (**A**) Cell morphological change. Senescent (S) HDFs were plated in 6-well plates at a density of 6×10⁴ cell per well and non-senescent (NS) HDFs were plated in 6-well plates at a density of 8×10⁴ cell per well. And then, the HDFs were treated with DMSO or R406 (2, 10 μM) for one day. Images were randomly captured by inverted microscopy (scale bar: 100 μm). (**B–D**) Senescent and non-senescent HDFs were treated with DMSO or R406 (10 μM) for one day and then western blot assays were conducted to determine changing expression levels of apoptosis regulating factors. (**E**, **F**) Senescent and non-senescent HDFs were respectively treated with DMSO, R406 (10 μM), and staurosporine (100 nM) for one day and apoptosis assays with Annexin V/PI staining were conducted.

days or more on senescent cells to show effectiveness [17, 22, 28]. Thus, we examined the senolytic effects of R406 in comparison to ABT263 over an appropriate treatment time in the RS model of HDFs. For this purpose, we treated R406 (2 or 10 μM) and ABT263 (1 μM) for one or three days on HDFs. Interestingly, R406 induced greater expression of cleaved-caspase-9, -7, and -3 after one day of treatment than ABT263 did in senescent cells (Figure 3A–3C). The expression of cleaved-caspase-9 and -7 was at similar levels between R406 and ABT263 treatment after three days (Figure 3D–3F). In addition, morphological changes to cell shrinkage appeared from 3 h in R406-treated senescent cells, whereas ABT263 did not induce significant change as viewed with time-lapse cell imaging (Supplementary Video 1). The results indicate that R406 triggers a senolytic effect much faster than ABT263 or other senolytic drugs that have been studied [17, 22, 26, 28].

As in the example of the combination of dasatinib and quercetin in which senolytic effect is potentiated [17], we additionally tested the additive senolytic effect of R406 with ABT263. Interestingly, the expression of cleaved-caspase-7 was more induced by co-treating with R406 (2 μM or 10 μM) and ABT263 (1 μM) than by individual treatment of R406 or ABT263 (Figure 3G), which indicates that R406 and ABT263 might have different modes in cell death activation and R406 with combination of other senolytic drugs could potentiate senescent cell death selectively.

We next assessed the senolytic effect of R406 in stress-induced premature senescence (SIPS) model as shown that in the RS. Cellular senescence was induced by either etoposide (inducing DNA damage) or H_2O_2 (increasing ROS level), which was confirmed by the upregulation of cell cycle regulators p16 and p21 (Supplementary Figure 3B). R406 inhibited the cell viability of etoposide or H_2O_2-treated HDFs in dose-dependent manner (Supplementary Figure 3C). Moreover, R406 induced the expression of cleaved-caspase-9 and-7 in the stress-induced HDFs one day post drug treatment (Supplementary Figure 3D, 3E). The results indicate that R406 exhibits senolytic effect in various modalities of cellular senescence.

R406-induced ROS generation is associated with senescent cell death

Next, we examined how R406 triggers apoptosis in senescent cells. Recent studies show that R406 induces ROS-dependent apoptotic effects via Syk-dependent and independent mechanisms in glioma stem cells [29]. For that reason, we tested whether R406 induces apoptosis via ROS generation in senescent HDFs. R406 induced ROS levels in a dose-dependent manner

(Figure 4A). Notably, at 10 μM of R406, higher ROS levels were observed in senescent cells than in non-senescent cells (Figure 4A). However, R406 suppressed phosphorylation of Syk regardless of cell's senescence state (Supplementary Figure 5). In order to check the relationship between R406-mediated ROS generation and apoptosis of senescent cells, we tested the R406-induced apoptotic effect in the presence of an antioxidant, N-acetyl-L-cysteine (NAC). We confirmed that 25 mM of NAC reduced about 70% of R406-mediated ROS generation (Figure 4B). Interestingly, NAC reduced R406-induced cytotoxicity in senescent HDFs in a statistically significant manner (Figure 4C). However, the level of cleaved-caspase-9 and -7 was not changed in R406 treated senescent HDFs even in the presence of NAC (Figure 4D). These results indicate that R406-dependent ROS generation would be a factor in senescent cell death, even though it might not involve apoptosis in senescent cells.

R406 induces a senolytic effect via dual inhibition of FAK and p38 MAPK

Cell survival is regulated by various signal pathways that are controlled by protein kinases [30–35]. Previous studies showed that FAK, a key molecule for cell adhesion, is critical for cell survival; blocking the FAK pathway increases the loss of substrate adhesion and induction of apoptosis of anchorage-dependent cells [36, 37]. Notably, our observation regarding live cell imaging led us to hypothesize that R406 induces morphological change in senescent cells via decreased cell adhesion. To validate this hypothesis, we checked the phosphorylation of FAK after short-term exposure to senolytic drugs. R406 altered the phosphorylation of FAK levels only in senescent HDFs (Figure 5A), whereas ABT263 did not change the phosphorylation of FAK. (Figure 5B). We then examined whether R406 affects the apoptotic effect on senescent cells via FAK signaling. Senescent and non-senescent HDFs were treated with a DMSO or a FAK inhibitor, PF562771, for one day and the expression of cleaved-caspase-3 and staining of annexin V/PI measured. Contrary to our expectations, the FAK inhibitor did not induce either the cleaved-caspase-3 expression or an apoptotic effect in HDFs (Figure 5C–5F). These results imply that R406-mediated FAK dephosphorylation would be one of the critical factors for inducing senescent cell death; however, FAK inactivation would not be a sole causality for the apoptosis of senescent cells.

Mitogen-activated protein kinases (ERK, JNK, and p38) and AKT mediate cell survival and death signals, which are stimulated by a diverse range of cytokine, growth factor, and chemical agents in mammalian cells [30–35]. Thus, we studied whether the senolytic effect of R406 is

related to the MAPKs and AKT signaling pathways. The results showed that phosphorylation of AKT, JNK, and ERK was inhibited by R406, regardless of cellular senescence. Interestingly, p38 phosphorylation was more inhibited by R406 in senescent cells than non-senescent cells (Figure 6A, 6B). However, a p38 inhibitor, SB202190, did not stimulate cleaved-caspase-9 and -3 (Figure 6C, 6D). These results also indicate that the R406-mediated p38 dephosphorylation might be associated with senescent cell death, but p38 inactivation would not be the only reason for apoptosis of senescent cells.

Although R406 induced FAK or p38 dephosphorylation, the inactivation of either kinase would not be enough to trigger apoptosis of senescent cells (Figures 5 and 6). Thus, we tested whether the R406- induced senolytic effect is mediated by the dual mechanisms of FAK and p38 at the same time. Indeed, the expression of cleaved-caspase-9 was induced only in senescent cells via co-treatment of PF562771 and SB202190 (Figure 7A). These results suggest that R406 induces apoptotic cell death of senescent cells by inactivation of multiple cell survival-related kinases including FAK and p38 MAPK.
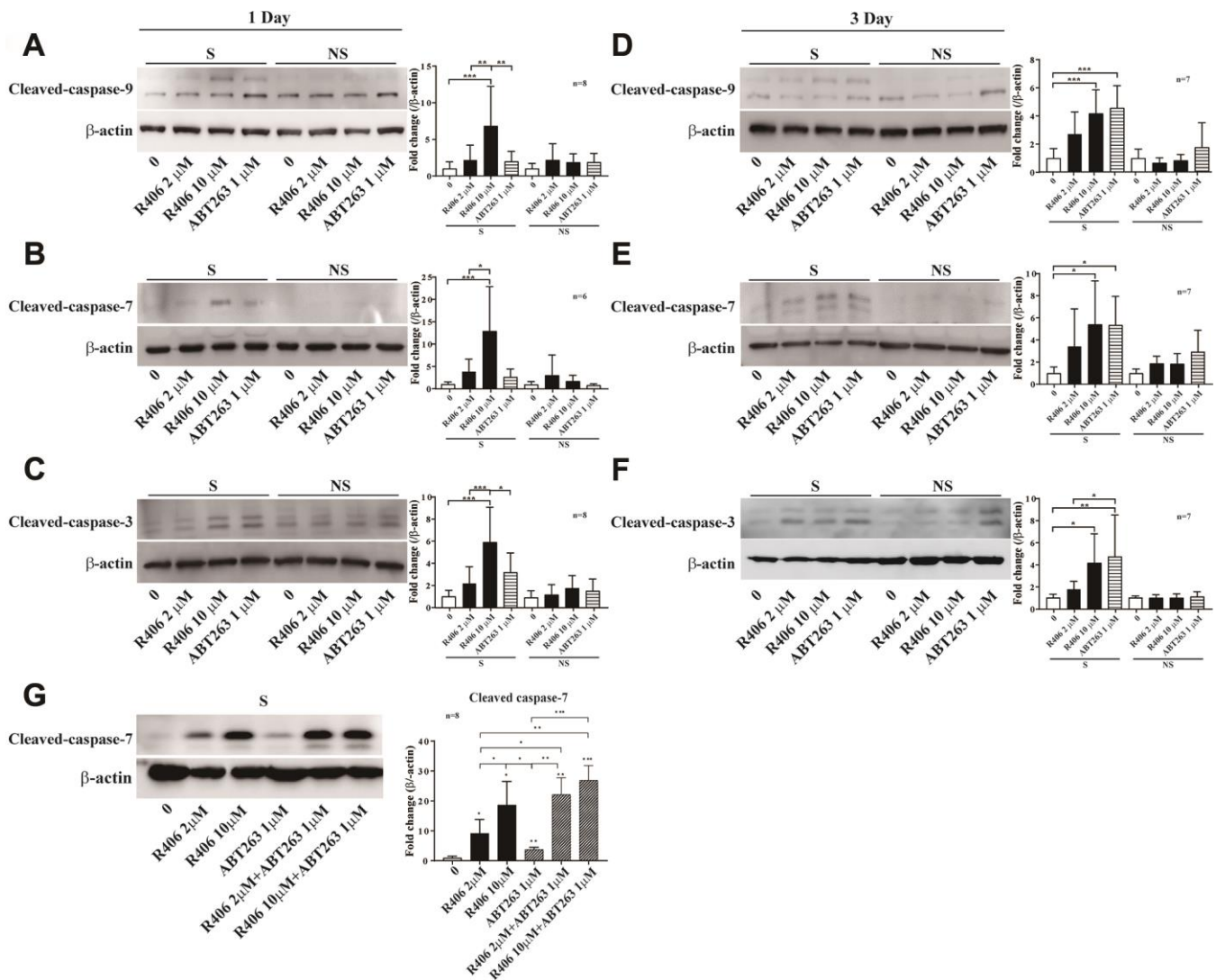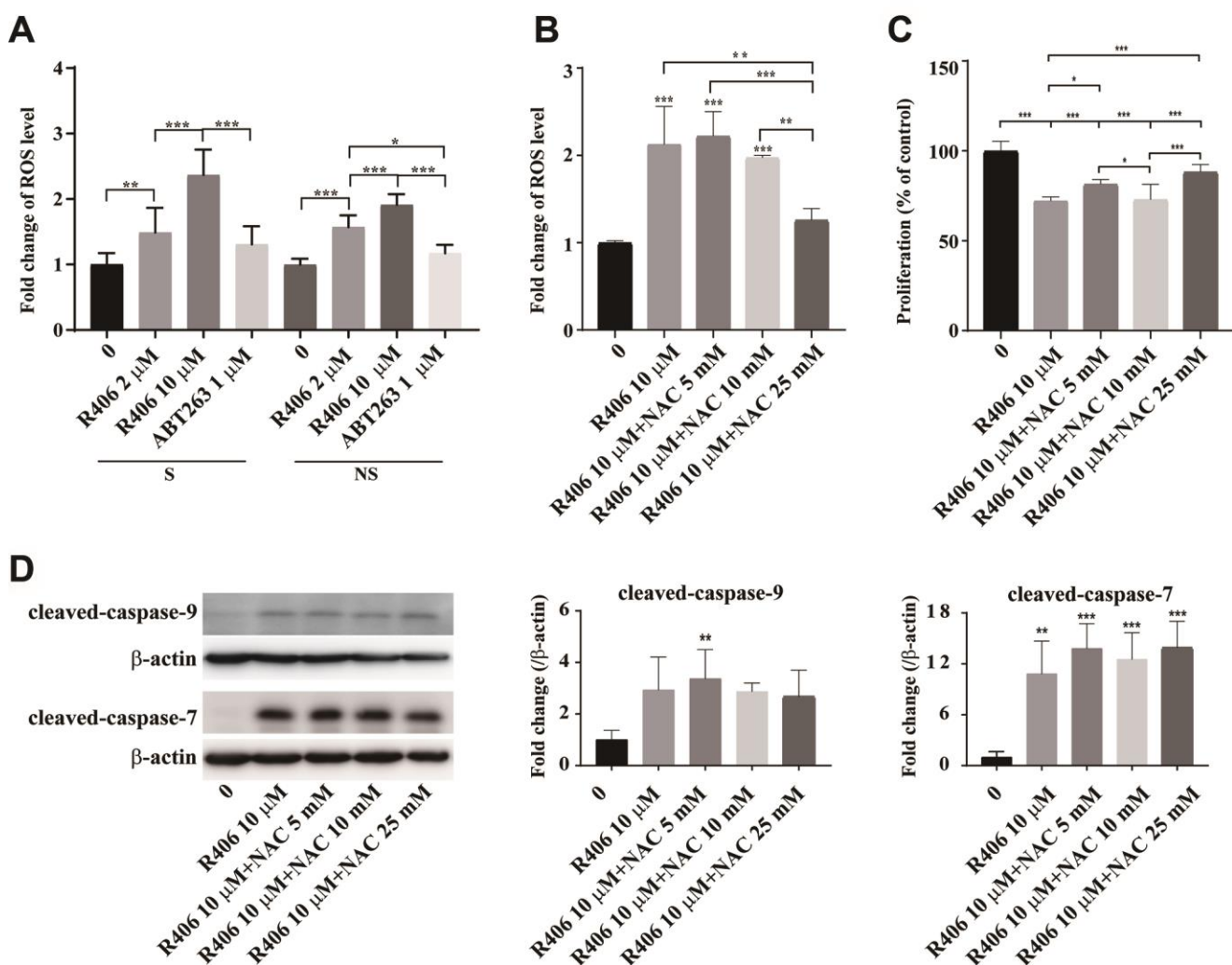

Figure 3. R406 induces cleavage of caspases in senescent HDFs. (**A**–**C**) Senescent (S) and non-senescent (NS) HDFs were treated with DMSO, R406 (2, 10 μM), and ABT263 (1 μM) for one day and then western blot assays using anti-caspase antibodies were conducted to determine senolytic effect by apoptosis. (**D**–**F**) Senescent and non-senescent HDFs were treated with DMSO, R406 (2, 10 μM), and ABT263 (1 μM) for three days and then monitored the level of cleaved-caspases by western blot analyses. (**G**) Senescent HDFs were respectively treated with single or combination of R406 and ABT263 for one day and then western blot assay with anti-caspase-7 antibody was conducted to determine apoptosis. *p<*0.05, **p<0.01, ***P<0.001.*

DISCUSSION

Selective clearance of senescent cells has been suggested to induce rejuvenation and longevity. In animal models, senolytic drugs have been shown to delay several age-associated disorders, to improve physical and cognitive function, and to extend lifespan [13, 14]. Because known senolytic drugs have limited diversity for their mode-of-action and affect change in a cell-type-specific manner [38], novel senolytic drugs are needed to improve efficacy and expend medical application against senescent cells.

This study demonstrated that R406 has several new aspects compared to other senolytic agents, beginning with its molecular mechanism for killing senescent cells. Resistance to apoptosis is one of the significant characteristics of senescent cells [2, 6, 7]. It is known that this resistance is associated with failure to suppress Bcl-2 activity [39] and, consequently, many senolytic agents target the Bcl-2 family-mediated anti-apoptotic pathway in senescent cells [40]. The R406 induced apoptosis pathway led to the increased expression of cleaved-caspase-9, -7, and -3 (Figure 3). This action by R406 is similar to other senolytic agents such as ABT263 (Supplementary Figure 4), quercetin, and A1331852 [22, 41, 42]. In contrast, R406 has no significant effect on expression of the Bcl-2 protein family (Figure 2).

Figure 4. R406 induces ROS generation. (**A**) Senescent (S) and non-senescent (NS) HDFs were treated with DMSO or R406 (10 μM) or ABT263 (1 μM) for one day and then ROS levels were detected with DHR123 staining with normalization by DNA contents. (**B**) Senescent and non-senescent HDFs were treated with R406 in the presence or absence of NAC for one day and then ROS levels were measured after DHR123 staining by flow cytometry. (**C**) Senescent HDFs were co-treated with R406 and NAC for one day and then CCK-1 assay were conducted to investigate cell viability. n = 8 (**D**) Senescent HDFs were co-treated with R406 and NAC for one day and then western blot assays using antibodies against caspase-9, and -7 were conducted. *p<0.05, **p<0.01, ***P<0.001*

To determine molecular pathways for R406-dependent cytotoxicity in senescent cells, we considered signals for cell survival, including the cell adhesion and MAPK pathways. FAK is a focal adhesion-associated protein kinase involved in cellular adhesion and spreading process, cell migration, and cell survival [7]. FAK expression and its phosphorylation for focal adhesion formation increased in senescent HDFs [8, 9]. In contrast, blocking the FAK pathway increases the loss of substrate adhesion and induction of apoptosis of anchorage-dependent cells [10–12]. In

our study, we observed that cellular morphological changes appeared from 5 h after R406 treatment (Supplementary Video 1). Phosphorylation at Tyr576/577 and Tyr397 of FAK in senescent HDFs was strongly inhibited by R406 compared to that in non-senescent HDF cells. Tyr397 of FAK is an auto-phosphorylation site for focal adhesion formation and Tyr576/577 is a Src-dependent phosphorylation site and related to apoptosis [8, 10]. We showed the inhibition of phosphorylation at Tyr397 and Tyr576/577 of FAK by R406 (Figure 5A), which
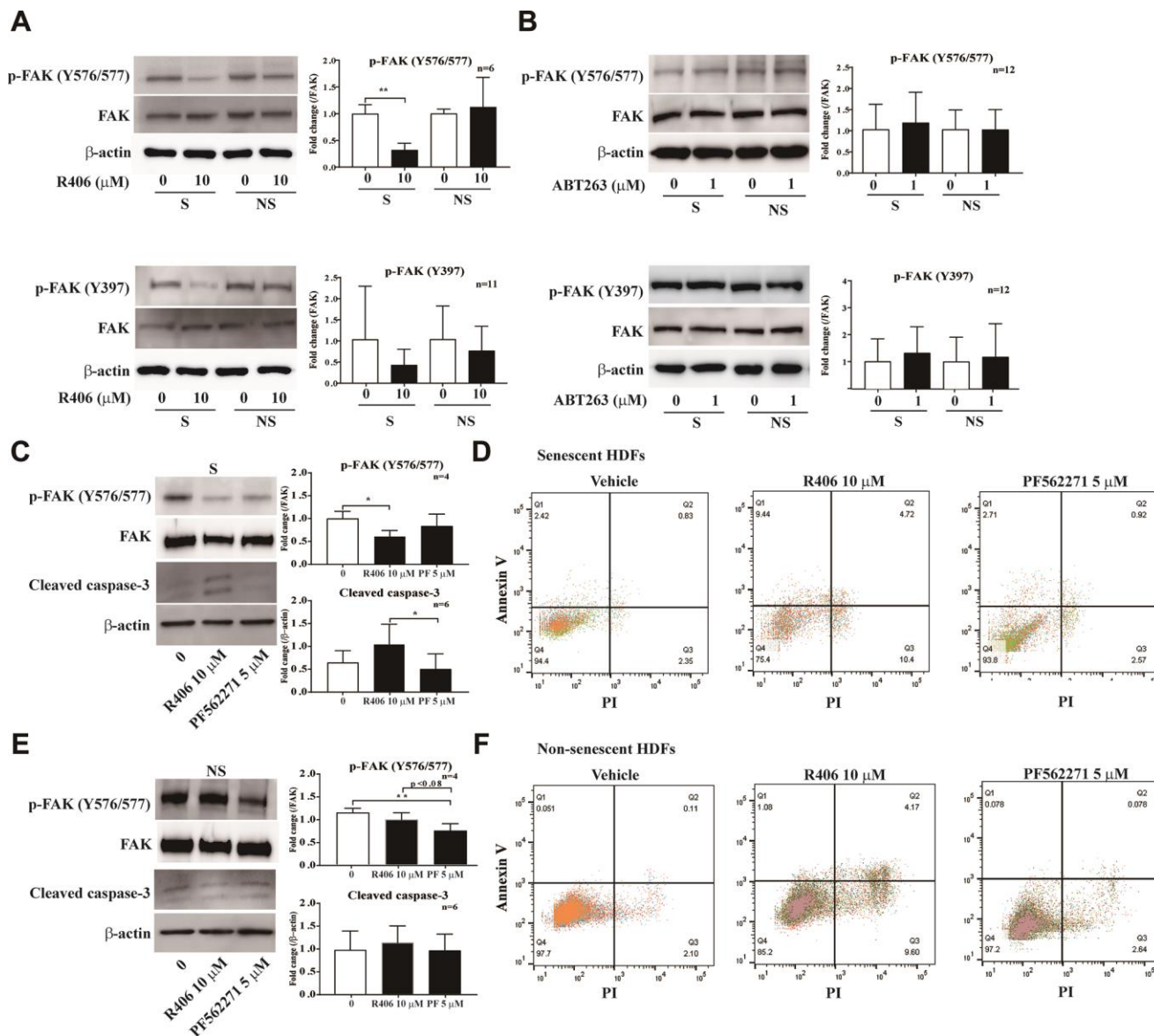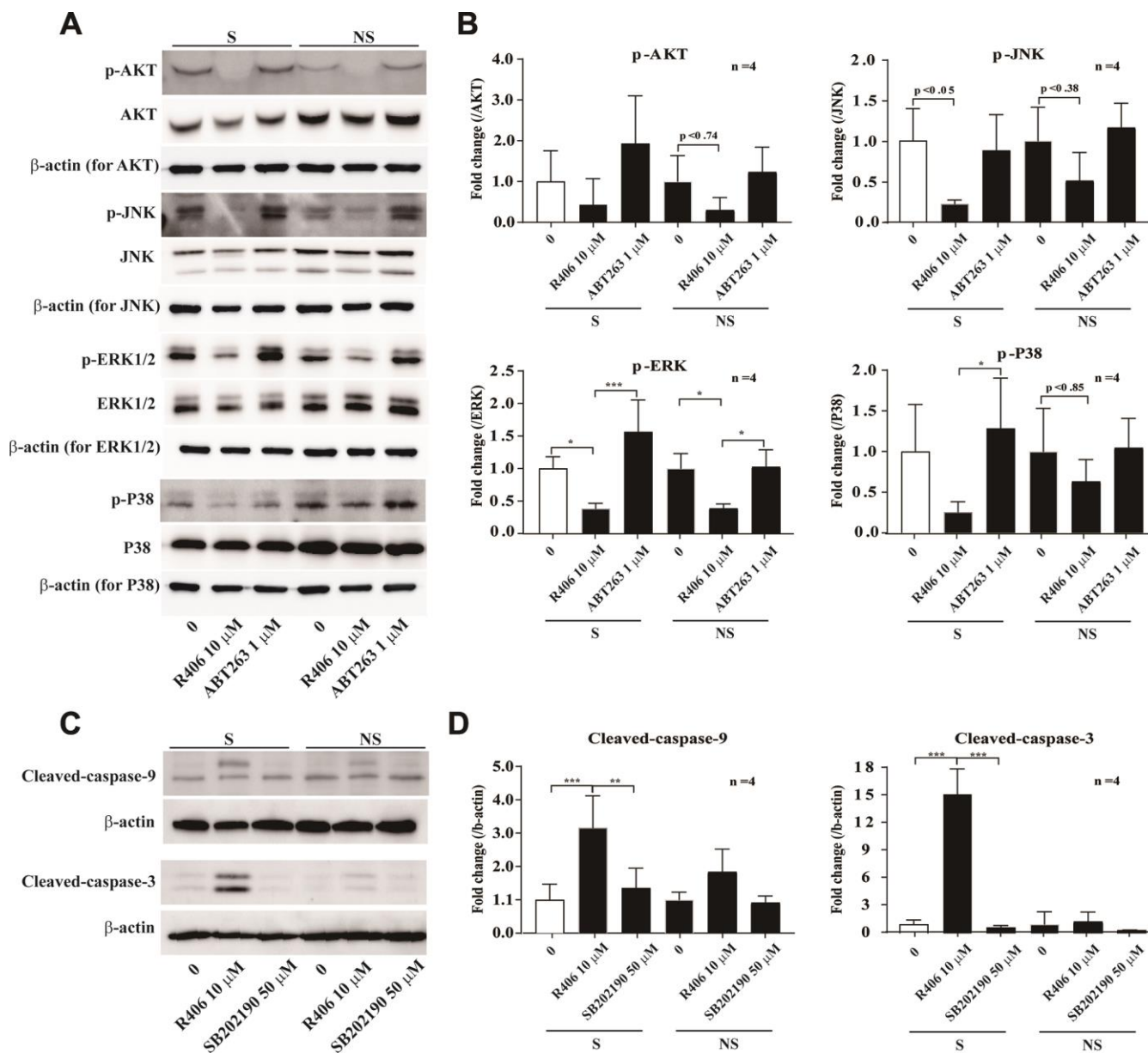

Figure 5. R406 inhibits phosphorylation of FAK in senescent HDFs more than non-senescent cells. (**A**, **B**) Senescent (S) and non-senescent (NS) HDFs were treated with R406 (10 μM, **A**), or ABT263 (1 μM, **B**) for 1 h and then western blot assays with anti-p-FAK and FAK antibodies. (**C**, **D**) Senescent HDFs were respectively treated with DMSO, R406 (10 μM), and PF562271 (5 μM) for one day and then western blot assay (anti-p-FAK and caspase-3, **C**) and apoptosis assay with Annexin V/PI staining (**D**) were conducted to determine senolytic effect. (**E**, **F**) Western blot (**E**) and apoptosis assay (**F**) with non-senescent HDFs as described in **C** and **D**. *$p<0.05$, **$p<0.01$, ***$P<0.001$.

indicated that R406 induces cellular morphological change and apoptosis via FAK inactivation. However, the FAK inhibitor (PF562271) alone did not induce either expression of cleaved caspase-3 or apoptotic effect in HDFs (Figure 5). These results imply that R406 would eliminate senescent HDF cells by weakening cell adhesion and inducing apoptosis through FAK inhibition, but R406-dependent FAK inactivation would not be the only trigger for inducing apoptosis in senescent cells.

Next, we checked whether R406 alters phosphorylation of JNK and p38. Among them, R406 strongly inhibited the phosphorylation of p38 in senescent cells, in contrast to its actions in non-senescent cells (Figure 6A and 6B). Similar to the FAK inhibitor, p38 inhibitor (SB202190) alone did not stimulate cleaved-caspase-9 and -3 (Figure 6C and 6D). This observation implies that R406-induced p38 dephosphorylation would also be associated with senescent cell death, but that p38 inactivation could not solely trigger apoptosis of
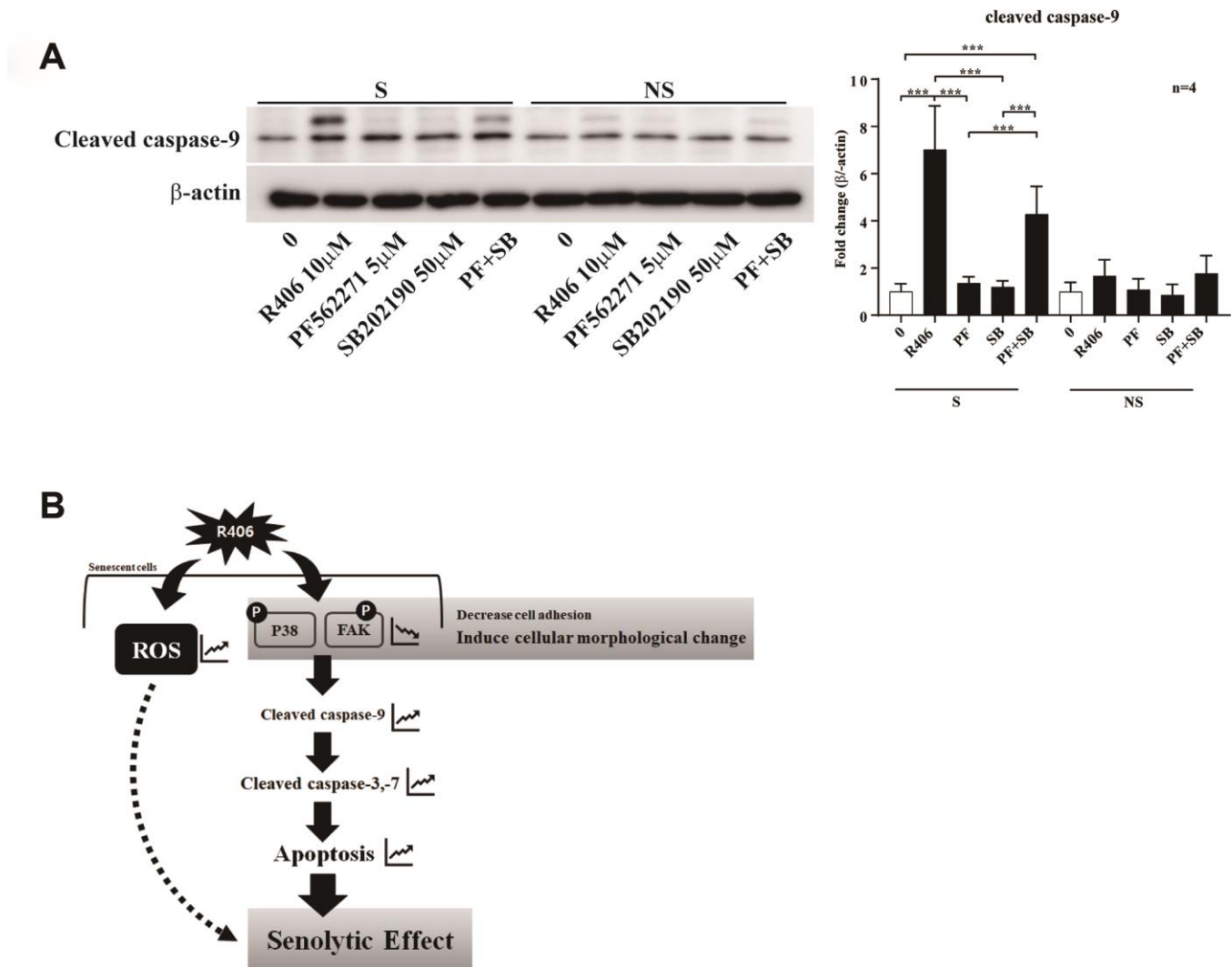

Figure 6. R406 inhibits phosphorylation of p38 MAPK in senescent HDFs more than non-senescent HDFs. (**A**, **B**) Senescent (S) and non-senescent (NS) HDFs were treated with DMSO, R406 (10 µM), and ABT263 (1 µM) for one day and western blot assays using anti-MAPKs antibodies were conducted. (**C**, **D**) Senescent HDFs were respectively treated with DMSO, R406 (10 µM), and SB202190 (p38 inhibitor, 50 µM) for one day. Then, western blot assays were conducted to determine triggering apoptosis by caspase cleavage. *p<0.05, **p<0.01, ***P<0.001.

senescent cells. Interestingly, co-treatment with the FAK inhibitor and p38 inhibitor resulted in the cleavage of caspase-9, specifically in senescent cells (Figure 7A). These observations together with R406-induced kinase inhibition allow us to propose a working model for R406 as a senolytic whereby the drug-induced cell death is mediated by inhibiting FAK and p38 activity as well as increasing ROS (Figure 7B).

In apoptotic cell death, various kinase pathways, including MAPKs and AKT, are involved. [31–34]. Not only that, FAK exists at the upstream or downstream of AKT signaling and MAPK pathway [43–45]. These mentioned kinases are related to anoikis which is

apoptosis induced by inappropriate cell-matrix interaction [46]. Previous studies demonstrated that anoikis was suppressed via a degradation of Bim and Bad by enhancing FAK, ERK, and AKT [47, 48]. We confirmed that R406 inhibits phosphorylation of AKT, ERK, and FAK (Figures 5 and 6). Thus, we anticipated that inactivation of FAK/ERK/AKT by R406 would increase the amount of Bim and Bad. As expect, R406 significantly induced the amount of Bim. Particularly, Bim level was slightly induced by R406 in non-senescent HDFs, but not as much as the senescent HDFs (Figure 2C). The results imply that R406 might induce the activation of anoikis in senescent cells and further studies about the process are waiting to be carried out.

Figure 7. R406 induces senolytic effects via blocking the phosphorylation of p38 MAPK and FAK simultaneously. (**A**) Senescent (S) and non-senescent (NS) HDFs were respectively treated with DMSO, R406 (10 μM), PF562271 (5 μM), and SB202190 (50 μM) for one day and then western blot assay with anti-caspase-9 antibody was conducted to determine apoptosis. (**B**) Proposed mechanism of senolytic effect by R406. R406-induced cell death is mediated by inhibiting FAK and p38 activity as well as increasing ROS. *p<0.05, **p<0.01, ***P<0.001.*

In terms of drug effectiveness, R406 can broaden the spectrum of senolytics in that R406 is effective in the RS model of genetically unmodified primary cells. In previous studies, typical senolytic agents (dasatinib, quercetin, ABT263, A1331852, and A1155463) were primarily studied in ionizing radiation-induced senescent cells, one of SIPS models [17, 22, 40, 49, 50]. Although RS and SIPS models share many common age-related cellular phenotypes like cell-cycle arrest, SA-β-gal induction or SASP increase, they also have distinct characteristics including patterns of protein expression [5]. Senolytic effects also present differently with senescence types [51]. Notwithstanding the limitation to verify the effectiveness of R406 in other cell types rather than HDFs as well as in an *in vivo* system, R406 could expand options for selecting effective combinations of senolytic drugs in various senescence contexts.

In conclusion, we demonstrate that R406 is a new class of senolytics that inhibits multiple cell survival signaling including FAK and p38 MAPK, which have been previously unrecognized in senolytic pathways. With diverse molecular mechanisms for eliminating senescent cells, R406 will be more effective in combination with senolytics targeting other anti-apoptotic pathways in senescent cells, which would become a valuable tool to overcome age-associated impairment.

MATERIALS AND METHODS

Cell lines and culture condition

Human diploid fibroblasts (HDFs) were obtained from the ATCC (PCS-201-010, Manassas, VA, USA). Cells were cultured in the growth media composed of DMEM (Welgene, Korea) supplemented with 10% FBS (Welgene), Antibiotic-Antimycotic solution (100 units/ml penicillin, 100 ug/ml streptomycin and 250 ng/ml amphotericin B, Welgene) at 37 °C in 5% CO_2 incubator. We used senescent cells of which the population doubling time (DT) is more than 14 days and non-senescent cells of which DT is less than one days [25]. We used SIPS models of which non-senescent HDFs were treated with 20 μM etoposide for two days, or treated with 400 μM H_2O_2 for six days.

Drug preparation

Drugs were purchased from the following: NVP-BHG712 (S2202), AZD (S7106), CCT129202 (S1519), Nintedanib (S1010), R406 (S2194), Axitinib (S1005), Bosutinib (S1014), selumetinib (S1008), Navitoclax (ABT263, S1001), PF561772 (S2890, FAK inhibitor), and SB202190 (S1077, P38 inhibitor) from Selleckchem (Houston, TX, USA). Staurosporine (S9300), etoposide

(E1383), and H_2O_2 (216763) from Sigma-Aldrich (St. Louis, MO, USA). They were prepared 10 mM stock solution in DMSO. They were added in culture medium to obtain a suitable working solution. As a vehicle, DMSO as the same volume was added in culture medium. The stock solution was stored at -20 °C.

Cell viability assay

Cell viability was determined using water-soluble tetrazolium salt-based D-plus cell viability and cytotoxicity assay reagent (CCK-1 reagent, Dongin LS, Korea). Cells were seeded in the 96-well plate and respectively treated with 0.5, 1, 5, 10 and 20 μM of NBP-BHG712, AZD and CCT129202, and 1, 2, 5, 10 and 20 μM of nintedanib, R406 and axitinib, and 0.1, 0.5, 1, 2 and 4 μM of bosutinib, and 1, 10, 25, 50, and 75 μM of selumetinib for 24 hours in the growth media. Cells were treated with 0.1, 0.5, 1, 5, and 10 μM of ABT263 respectively for one day or three days. Cells were then treated with 10 μl CCK-1 reagent and incubated for 4 hours at 37 °C in 5% CO_2 incubator. After incubation, plates were read absorbance in 450 nm using the multi plate reader (Infinite M200PRO). In to check cell viability using the Hoechst 33342 staining, cells were seeded in the 24-well plate and respectively treated with 1, 2, 5, 10 and 20 μM of R406 for 24 hours in the growth media. Cells were then fix with 100% methanol for 10 min and washed with PBS. The Fixed cells were stained with 1 μg/ml Hoechst 33342 (#639, Immunochemistry Technologies, MN, USA) for 1 h and washed twice with PBS. Cell number was determined by measuring fluorescence intensity in Excitation/ Emission: 355 nm/460 nm using the multi plate reader (Infinite M200PRO).

SA-β-gal staining

To detect β-galactosidase activity, cells were stained using the senescence β-galactosidase staining kit (Cell Signaling, #9860) by following manufacturer's instructions. Development of blue color by β-galactosidase staining was estimated under a microscope.

Flow cytometry

Drug treated cells were harvested by trypsinization and resuspended in 1X Annexin V binding buffer (10 × Annexin V binding buffer: 0.1 M HEPES (pH 7.4), 1.4 M NaCl, 25 mM $CaCl_2$) containing 5 μl of Annexin V-Alexa fluor®350 conjugate (Thermo Fisher Scientific, A23202) and 2 μl of 100 μg/ml propidium iodide per $1x10^5$ cells in 100 μl, and then incubation for 15 min at the dark. After the incubation, add 400 μl 1X Annexin-binding buffer (final vol. 500 μl). The cells were analyzed by flow cytometry within 1 h.

Western blot analysis

Protein lysates were prepared by resuspending cell pellets in 2X laemmli sample (#161-0737, Bio-Rad Laboratories, Hercules, CA) buffer containing 5% β-mercaptoethanol. The protein lysates were separated by electrophoresis on SDS-PAGE and then electro-transferred onto Polyvinylidene difluoride (PVDF) membranes (Millipore Corp., Bradford, MA, USA). Detection of specific protein was carried out by enhanced chemiluminescence following the manufacturer's instructions (P90720, Millipore corporation, MA, USA). We used the following primary antibodies: Caspase-9 (#9503, #7237), Caspase-8 (#9746), Caspase-7 (#8438), Caspase-3 (#9664), Bak (#3814), Bax (#2772), Bcl-xl (#2762), p-AKT (#4058), AKT (#2967), p-ERK (#4376), ERK (#4695), p-P38 (#9216), P38 (#8690), p-JNK (#9255), JNK (#9258), p-SYK (#2710), and SYK (#2712) were purchased from C*ell Signaling* Technology, *Inc.*. PARP-1 (sc-74470) and β-actin (sc-47778) were purchased from Santa Cruz Biotechnology, Inc.. p-FAK(Y576/577) (ab76244), p21 (ab7960) were purchased from Abcam. p-FAK(Y397) (611722), FAK (611008), and p16 (551154) were purchased from BD Biosciences. Densitometry analyses were performed using Image J software.

Time-lapse imaging

Time-lapse images were captured using Axio-Observer Z1 microscopy (Zeiss) under incubating in PeCon microscopy incubator (PeCon GmbH) at 37°C and 5% CO_2. The cell images were captured with $10 \times$ objective in every 20 min for about 1.5 days to monitor cellular morphological change event.

Detection of ROS generation

Cell were incubated with 10 μM dihydrorhodamine 123 (DHR123, Biotium, CA, USA) for 1 h at 37°C and then washed twice with phosphate buffered saline (PBS), and ROS content was measured in excitation/emission: 500 nm/536 nm using a multimode plate reader (Infinite200 PRO, Tecan, Switzerland). To normalize ROS-derived fluorescence intensity with cell number, DNA content of the ROS measured cells was estimated. Cells were stained with 1 μg/ml Hoechst 33342 (#639, Immunochemistry Technologies, MN, USA) for 1 h and washed twice with PBS. Cell number was determined by measuring fluorescence intensity in Excitation/Emission: 355 nm/460 nm using the plate reader. ROS levels were calculated by normalizing DHR123-stained values with Hoechst 33342-stained value. In the analysis using flow cytometry, drug treated cells were harvested by trypsinization and re-suspended in complete growth media adding 10 μM DHR123. The cells were incubated for 1 h at 37°C followed by washing twice with PBS, and then analyzed by flow cytometry within 1 h. The mean ± S.D. from four replicates was determined for each experimental group.

Statistical analyses

All data were analyzed using ANOVA with Graphpad Prism 7 software. Post-hoc analyses were completed with Tukey's Multiple comparison test with p<0.05 significance. DATA represent mean ± S.D. (*p<0.05*, **p<0.01*, ***p<0.001*).

AUTHOR CONTRIBUTIONS

YSL and HJC conceived of and designed the experiments. HJC, EJY, JTP, ECK, KJJ and YSL performed the experiments and analyzed the data. All authors contributed to write and edited the paper.

REFERENCES

1. McHugh D, Gil J. Senescence and aging: Causes, consequences, and therapeutic avenues. J Cell Biol. 2018; 217:65–77.
   https://doi.org/10.1083/jcb.201708092
   PMID:29114066

2. López-Otín C, Blasco MA, Partridge L, Serrano M, Kroemer G. The hallmarks of aging. Cell. 2013; 153:1194–217.
   https://doi.org/10.1016/j.cell.2013.05.039
   PMID:23746838

3. van Deursen JM. The role of senescent cells in ageing. Nature. 2014; 509:439–46.
   https://doi.org/10.1038/nature13193
   PMID:24848057

4. Di Leonardo A, Linke SP, Clarkin K, Wahl GM. DNA damage triggers a prolonged p53-dependent G1 arrest and long-term induction of Cip1 in normal human fibroblasts. Genes Dev. 1994; 8:2540–51.

https://doi.org/10.1101/gad.8.21.2540
PMID:7958916

5. Mária J, Ingrid Ž. Effects of bioactive compounds on senescence and components of senescence associated secretory phenotypes in vitro. Food Funct. 2017; 8:2394–418.
https://doi.org/10.1039/C7FO00161D
PMID:28665427

6. Suh Y, Lee KA, Kim WH, Han BG, Vijg J, Park SC. Aging alters the apoptotic response to genotoxic stress. Nat Med. 2002; 8:3–4.
https://doi.org/10.1038/nm0102-3
PMID:11786880

7. Yeo EJ, Hwang YC, Kang CM, Choy HE, Park SC. Reduction of UV-induced cell death in the human senescent fibroblasts. Mol Cells. 2000; 10:415–22.
PMID:10987139

8. Sedelnikova OA, Horikawa I, Zimonjic DB, Popescu NC, Bonner WM, Barrett JC. Senescing human cells and ageing mice accumulate DNA lesions with unrepairable double-strand breaks. Nat Cell Biol. 2004; 6:168–70.
https://doi.org/10.1038/ncb1095 PMID:14755273

9. Rodier F, Coppé JP, Patil CK, Hoeijmakers WA, Muñoz DP, Raza SR, Freund A, Campeau E, Davalos AR, Campisi J. Persistent DNA damage signalling triggers senescence-associated inflammatory cytokine secretion. Nat Cell Biol. 2009; 11:973–79.
https://doi.org/10.1038/ncb1909
PMID:19597488

10. Storer M, Mas A, Robert-Moreno A, Pecoraro M, Ortells MC, Di Giacomo V, Yosef R, Pilpel N, Krizhanovsky V, Sharpe J, Keyes WM. Senescence is a developmental mechanism that contributes to embryonic growth and patterning. Cell. 2013; 155:1119–30.
https://doi.org/10.1016/j.cell.2013.10.041
PMID:24238961

11. Muñoz-Espín D, Cañamero M, Maraver A, Gómez-López G, Contreras J, Murillo-Cuesta S, Rodríguez-Baeza A, Varela-Nieto I, Ruberte J, Collado M, Serrano M. Programmed cell senescence during mammalian embryonic development. Cell. 2013; 155:1104–18.
https://doi.org/10.1016/j.cell.2013.10.019
PMID:24238962

12. Demaria M, Ohtani N, Youssef SA, Rodier F, Toussaint W, Mitchell JR, Laberge RM, Vijg J, Van Steeg H, Dollé ME, Hoeijmakers JH, de Bruin A, Hara E, Campisi J. An essential role for senescent cells in optimal wound healing through secretion of PDGF-AA. Dev Cell. 2014; 31:722–33.
https://doi.org/10.1016/j.devcel.2014.11.012
PMID:25499914

13. Xu M, Pirtskhalava T, Farr JN, Weigand BM, Palmer AK, Weivoda MM, Inman CL, Ogrodnik MB, Hachfeld CM, Fraser DG, Onken JL, Johnson KO, Verzosa GC, et al. Senolytics improve physical function and increase lifespan in old age. Nat Med. 2018; 24:1246–56.
https://doi.org/10.1038/s41591-018-0092-9
PMID:29988130

14. Baker DJ, Wijshake T, Tchkonia T, LeBrasseur NK, Childs BG, van de Sluis B, Kirkland JL, van Deursen JM. Clearance of p16Ink4a-positive senescent cells delays ageing-associated disorders. Nature. 2011; 479:232–36.
https://doi.org/10.1038/nature10600
PMID:22048312

15. Fuhrmann-Stroissnigg H, Ling YY, Zhao J, McGowan SJ, Zhu Y, Brooks RW, Grassi D, Gregg SQ, Stripay JL, Dorronsoro A, Corbo L, Tang P, Bukata C, et al. Identification of HSP90 inhibitors as a novel class of senolytics. Nat Commun. 2017; 8:422.
https://doi.org/10.1038/s41467-017-00314-z
PMID:28871086

16. Kim EC, Kim JR. Senotherapeutics: emerging strategy for healthy aging and age-related disease. BMB Rep. 2019; 52:47–55.
https://doi.org/10.5483/BMBRep.2019.52.1.293
PMID:30526770

17. Zhu Y, Tchkonia T, Pirtskhalava T, Gower AC, Ding H, Giorgadze N, Palmer AK, Ikeno Y, Hubbard GB, Lenburg M, O'Hara SP, LaRusso NF, Miller JD, et al. The Achilles' heel of senescent cells: from transcriptome to senolytic drugs. Aging Cell. 2015; 14:644–58.
https://doi.org/10.1111/acel.12344
PMID:25754370

18. Roos CM, Zhang B, Palmer AK, Ogrodnik MB, Pirtskhalava T, Thalji NM, Hagler M, Jurk D, Smith LA, Casaclang-Verzosa G, Zhu Y, Schafer MJ, Tchkonia T, et al. Chronic senolytic treatment alleviates established vasomotor dysfunction in aged or atherosclerotic mice. Aging Cell. 2016; 15:973–77.
https://doi.org/10.1111/acel.12458
PMID:26864908

19. Palmer AK, Xu M, Zhu Y, Pirtskhalava T, Weivoda MM, Hachfeld CM, Prata LG, van Dijk TH, Verkade E, Casaclang-Verzosa G, Johnson KO, Cubro H, Doornebal EJ, et al. Targeting senescent cells alleviates obesity-induced metabolic dysfunction. Aging Cell. 2019; 18:e12950.
https://doi.org/10.1111/acel.12950
PMID:30907060

20. Jeon OH, Kim C, Laberge RM, Demaria M, Rathod S, Vasserot AP, Chung JW, Kim DH, Poon Y, David N, Baker DJ, van Deursen JM, Campisi J, Elisseeff JH. Local clearance of senescent cells attenuates the development of post-traumatic osteoarthritis and

creates a pro-regenerative environment. Nat Med. 2017; 23:775–81.
https://doi.org/10.1038/nm.4324
PMID:28436958

21. Justice JN, Nambiar AM, Tchkonia T, LeBrasseur NK, Pascual R, Hashmi SK, Prata L, Masternak MM, Kritchevsky SB, Musi N, Kirkland JL. Senolytics in idiopathic pulmonary fibrosis: results from a first-in-human, open-label, pilot study. EBioMedicine. 2019; 40:554–63.
https://doi.org/10.1016/j.ebiom.2018.12.052
PMID:30616998

22. Zhu Y, Tchkonia T, Fuhrmann-Stroissnigg H, Dai HM, Ling YY, Stout MB, Pirtskhalava T, Giorgadze N, Johnson KO, Giles CB, Wren JD, Niedernhofer LJ, Robbins PD, Kirkland JL. Identification of a novel senolytic agent, navitoclax, targeting the Bcl-2 family of anti-apoptotic factors. Aging Cell. 2016; 15:428–35.
https://doi.org/10.1111/acel.12445
PMID:26711051

23. Baar MP, Brandt RMC, Putavet DA, Klein JDD, Derks KWJ, Bourgeois BRM, Stryeck S, Rijksen Y, van Willigenburg H, Feijtel DA, van der Pluijm I, Essers J, van Cappellen WA, et al. Targeted Apoptosis of Senescent Cells Restores Tissue Homeostasis in Response to Chemotoxicity and Aging. Cell. 2017; 169:132–147.e16.
https://doi.org/10.1016/j.cell.2017.02.031
PMID:28340339

24. Kang HT, Park JT, Choi K, Choi HJ, Jung CW, Kim GR, Lee YS, Park SC. Chemical screening identifies ROCK as a target for recovering mitochondrial function in Hutchinson-Gilford progeria syndrome. Aging Cell. 2017; 16:541–50.
https://doi.org/10.1111/acel.12584
PMID:28317242

25. Kang HT, Park JT, Choi K, Kim Y, Choi HJ, Jung CW, Lee YS, Park SC. Chemical screening identifies ATM as a target for alleviating senescence. Nat Chem Biol. 2017; 13:616–23.
https://doi.org/10.1038/nchembio.2342
PMID:28346404

26. Kirkland JL, Tchkonia T, Zhu Y, Niedernhofer LJ, Robbins PD. The Clinical Potential of Senolytic Drugs. J Am Geriatr Soc. 2017; 65:2297–301.
https://doi.org/10.1111/jgs.14969
PMID:28869295

27. Chang J, Wang Y, Shao L, Laberge RM, Demaria M, Campisi J, Janakiraman K, Sharpless NE, Ding S, Feng W, Luo Y, Wang X, Aykin-Burns N, et al. Clearance of senescent cells by ABT263 rejuvenates aged hematopoietic stem cells in mice. Nat Med. 2016; 22:78–83.
https://doi.org/10.1038/nm.4010
PMID:26657143

28. Pan J, Li D, Xu Y, Zhang J, Wang Y, Chen M, Lin S, Huang L, Chung EJ, Citrin DE, Wang Y, Hauer-Jensen M, Zhou D, Meng A. Inhibition of Bcl-2/xl With ABT-263 Selectively Kills Senescent Type II Pneumocytes and Reverses Persistent Pulmonary Fibrosis Induced by Ionizing Radiation in Mice. Int J Radiat Oncol Biol Phys. 2017; 99:353–61.
https://doi.org/10.1016/j.ijrobp.2017.02.216
PMID:28479002

29. Sun S, Xue D, Chen Z, Ou-Yang Y, Zhang J, Mai J, Gu J, Lu W, Liu X, Liu W, Sheng L, Lu B, Lin Y, et al. R406 elicits anti-Warburg effect via Syk-dependent and -independent mechanisms to trigger apoptosis in glioma stem cells. Cell Death Dis. 2019; 10:358.
https://doi.org/10.1038/s41419-019-1587-0
PMID:31043589

30. Danen EH, Sonneveld P, Sonnenberg A, Yamada KM. Dual stimulation of Ras/mitogen-activated protein kinase and RhoA by cell adhesion to fibronectin supports growth factor-stimulated cell cycle progression. J Cell Biol. 2000; 151:1413–22.
https://doi.org/10.1083/jcb.151.7.1413
PMID:11134071

31. Ihermann-Hella A, Lume M, Miinalainen IJ, Pirttiniemi A, Gui Y, Peränen J, Charron J, Saarma M, Costantini F, Kuure S. Mitogen-activated protein kinase (MAPK) pathway regulates branching by remodeling epithelial cell adhesion. PLoS Genet. 2014; 10:e1004193.
https://doi.org/10.1371/journal.pgen.1004193
PMID:24603431

32. Zhang W, Liu HT. MAPK signal pathways in the regulation of cell proliferation in mammalian cells. Cell Res. 2002; 12:9–18.
https://doi.org/10.1038/sj.cr.7290105
PMID:11942415

33. Haston S, Pozzi S, Carreno G, Manshaei S, Panousopoulos L, Gonzalez-Meljem JM, Apps JR, Virasami A, Thavaraj S, Gutteridge A, Forshew T, Marais R, Brandner S, et al. MAPK pathway control of stem cell proliferation and differentiation in the embryonic pituitary provides insights into the pathogenesis of papillary craniopharyngioma. Development. 2017; 144:2141–52.
https://doi.org/10.1242/dev.150490
PMID:28506993

34. Yamaguchi H, Wang HG. The protein kinase PKB/Akt regulates cell survival and apoptosis by inhibiting Bax conformational change. Oncogene. 2001; 20:7779–86.
https://doi.org/10.1038/sj.onc.1204984
PMID:11753656

35. Reddy P, Liu L, Ren C, Lindgren P, Boman K, Shen Y, Lundin E, Ottander U, Rytinki M, Liu K. Formation of E-cadherin-mediated cell-cell adhesion activates AKT and mitogen activated protein kinase via phosphatidylinositol 3 kinase and ligand-independent activation of epidermal growth factor receptor in ovarian cancer cells. Mol Endocrinol. 2005; 19:2564–78.
https://doi.org/10.1210/me.2004-0342
PMID:15928314

36. Kong D, Chen F, Sima NI. Inhibition of focal adhesion kinase induces apoptosis in bladder cancer cells via Src and the phosphatidylinositol 3-kinase/Akt pathway. Exp Ther Med. 2015; 10:1725–31.
https://doi.org/10.3892/etm.2015.2745
PMID:26640543

37. Lu Q, Rounds S. Focal adhesion kinase and endothelial cell apoptosis. Microvasc Res. 2012; 83:56–63.
https://doi.org/10.1016/j.mvr.2011.05.003
PMID:21624380

38. Blagosklonny MV. Paradoxes of senolytics. Aging (Albany NY). 2018; 10:4289–93.
https://doi.org/10.18632/aging.101750
PMID:30594910

39. Wang E. Senescent human fibroblasts resist programmed cell death, and failure to suppress bcl2 is involved. Cancer Res. 1995; 55:2284–92.
PMID:7757977

40. Kirkland JL, Tchkonia T. Cellular Senescence: A Translational Perspective. EBioMedicine. 2017; 21:21–28.
https://doi.org/10.1016/j.ebiom.2017.04.013
PMID:28416161

41. Kovacovicova K, Skolnaja M, Heinmaa M, Mistrik M, Pata P, Pata I, Bartek J, Vinciguerra M. Senolytic Cocktail Dasatinib+Quercetin (D+Q) Does Not Enhance the Efficacy of Senescence-Inducing Chemotherapy in Liver Cancer. Front Oncol. 2018; 8:459.
https://doi.org/10.3389/fonc.2018.00459
PMID:30425964

42. Zhu Y, Doornebal EJ, Pirtskhalava T, Giorgadze N, Wentworth M, Fuhrmann-Stroissnigg H, Niedernhofer LJ, Robbins PD, Tchkonia T, Kirkland JL. New agents that target senescent cells: the flavone, fisetin, and the BCL-X$_L$ inhibitors, A1331852 and A1155463. Aging (Albany NY). 2017; 9:955–63.
https://doi.org/10.18632/aging.101202
PMID:28273655

43. Huang C, Jacobson K, Schaller MD. MAP kinases and cell migration. J Cell Sci. 2004; 117:4619–28.
https://doi.org/10.1242/jcs.01481
PMID:15371522

44. Wu YJ, Neoh CA, Tsao CY, Su JH, Li HH. Sinulariolide Suppresses Human Hepatocellular Carcinoma Cell Migration and Invasion by Inhibiting Matrix Metalloproteinase-2/-9 through MAPKs and PI3K/Akt Signaling Pathways. Int J Mol Sci. 2015; 16:16469–82.
https://doi.org/10.3390/ijms160716469
PMID:26204832

45. Kanteti R, Batra SK, Lennon FE, Salgia R. FAK and paxillin, two potential targets in pancreatic cancer. Oncotarget. 2016; 7:31586–601.
https://doi.org/10.18632/oncotarget.8040
PMID:26980710

46. Frisch SM, Screaton RA. Anoikis mechanisms. Curr Opin Cell Biol. 2001; 13:555–62.
https://doi.org/10.1016/S0955-0674(00)00251-9
PMID:11544023

47. Paoli P, Giannoni E, Chiarugi P. Anoikis molecular pathways and its role in cancer progression. Biochim Biophys Acta. 2013; 1833:3481–98.
https://doi.org/10.1016/j.bbamcr.2013.06.026
PMID:23830918

48. Haun F, Neumann S, Peintner L, Wieland K, Habicht J, Schwan C, Østevold K, Koczorowska MM, Biniossek M, Kist M, Busch H, Boerries M, Davis RJ, et al. Identification of a novel anoikis signalling pathway using the fungal virulence factor gliotoxin. Nat Commun. 2018; 9:3524.
https://doi.org/10.1038/s41467-018-05850-w
PMID:30166526

49. Wang Y, Meng A, Zhou D. Inhibition of phosphatidylinositol 3-kinase uncouples H2O2-induced senescent phenotype and cell cycle arrest in normal human diploid fibroblasts. Exp Cell Res. 2004; 298:188–96.
https://doi.org/10.1016/j.yexcr.2004.04.012
PMID:15242773

50. Hwang ES, Yoon G, Kang HT. A comparative analysis of the cell biology of senescence and aging. Cell Mol Life Sci. 2009; 66:2503–24.
https://doi.org/10.1007/s00018-009-0034-2
PMID:19421842

51. Pascal T, Debacq-Chainiaux F, Chrétien A, Bastin C, Dabée AF, Bertholet V, Remacle J, Toussaint O. Comparison of replicative senescence and stress-induced premature senescence combining differential display and low-density DNA arrays. FEBS Lett. 2005; 579:3651–59.
https://doi.org/10.1016/j.febslet.2005.05.056
PMID:15963989

Supplementary Figures
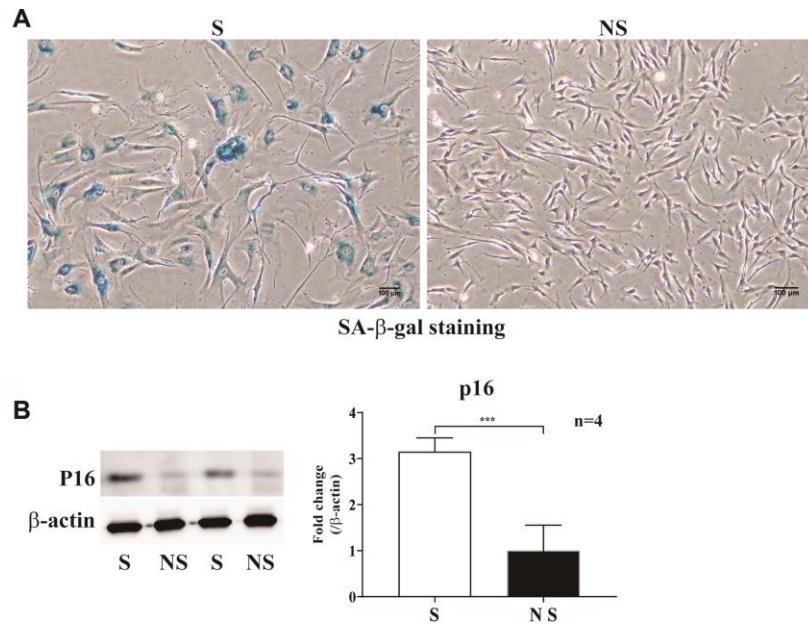
Supplementary Figure 1. Characterizing senescent and non-senescent HDFs. (**A**) Senescent cells increase SA-β-gal activity. Representative photomicrographs of SA-β-gal staining for non-senescent cells (NS) or senescent cells (S) are presented (scale bar: 100 μm). (**B**) Increasing p16 in senescent HDFs was determined by western blot analysis. *p<0.05, **p<0.01, ***P<0.001 compared to senescent HDFs.
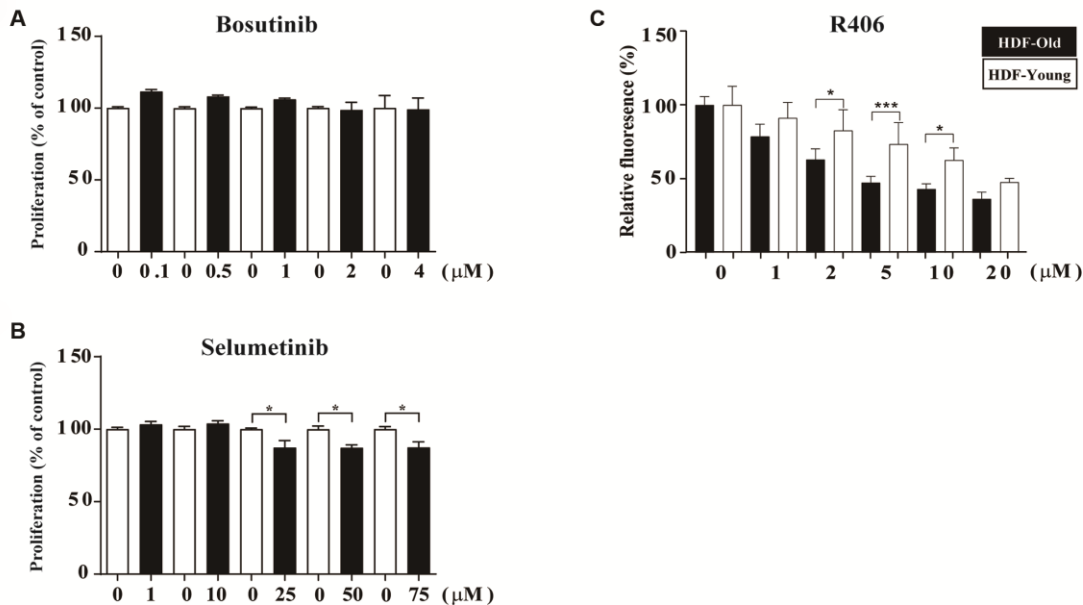

Supplementary Figure 2. Bosutinib and Selumetinib did not show senolytic effects in senescent cells. Senescent HDFs were respectively treated with DMSO (white bar), (**A**) Bosutinib (0.1, 0.5, 1, 2, 4 μM; black bar), and (**B**) Selumetinib (1, 10, 25, 50, 75 μM; black bar) for one day and then CCK-1 assays were conducted to investigate cell viability. (**C**) Senescent HDFs (HDF-Old) and non-senescent HDFs (HDF-Young) were treated with R406 (1, 2, 5, 10, 20 μM), and then, cell number was detected with Hoechst 33342 staining. n = 12, *p<0.05, **p<0.01, ***P<0.001.
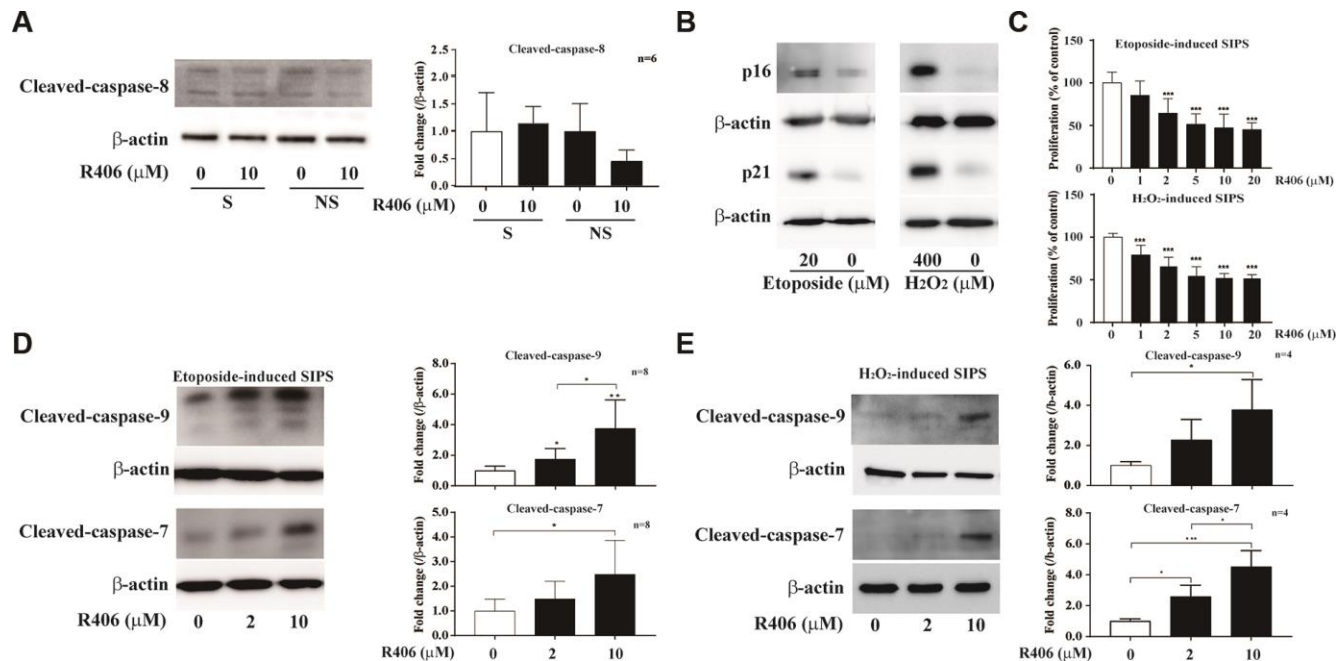
Supplementary Figure 3. R406 was not affect caspase-8 activity in senescent HDFs. (**A**) Senescent (S) and non-senescent (NS) HDFs were treated with DMSO and/or R406 (10 μM) for one day and then western blot assays were conducted with anti-cleaved caspase-8. (**B**) Non-senescent HDFs were treated with 20 μM etoposide for two days (left panel), and non-senescent HDFs were treated with 400 μM H_2O_2 for six days (right panel) and then western blot assays were conducted with anti-p16 and anti-p21. (**C**) 20 μM etoposide induced HDFs for two days were treated with DMSO and/or R406 (1, 2, 5, 10, 20 μM) for one day (upper panel), and 400 μM H_2O_2 induced HDFs for six days were treated with DMSO and/or R406 (1, 2, 5, 10, 20 μM) for one day (lower panel) and then CCK-1 assays were conducted to investigate cell viability. (**D**) Etoposide-induced SIPS were treated with DMSO and/or R406 (2, 10 μM) for one day and then western blot assays were conducted with anti-cleaved caspase-9, and -7. (**E**) H_2O_2-induced SIPS were treated with DMSO and/or R406 (2, 10 μM) for one day and then western blot assays were conducted with anti-cleaved caspase-9, and -7. *$p<0.05$, **$p<0.01$, ***$P<0.001$.*
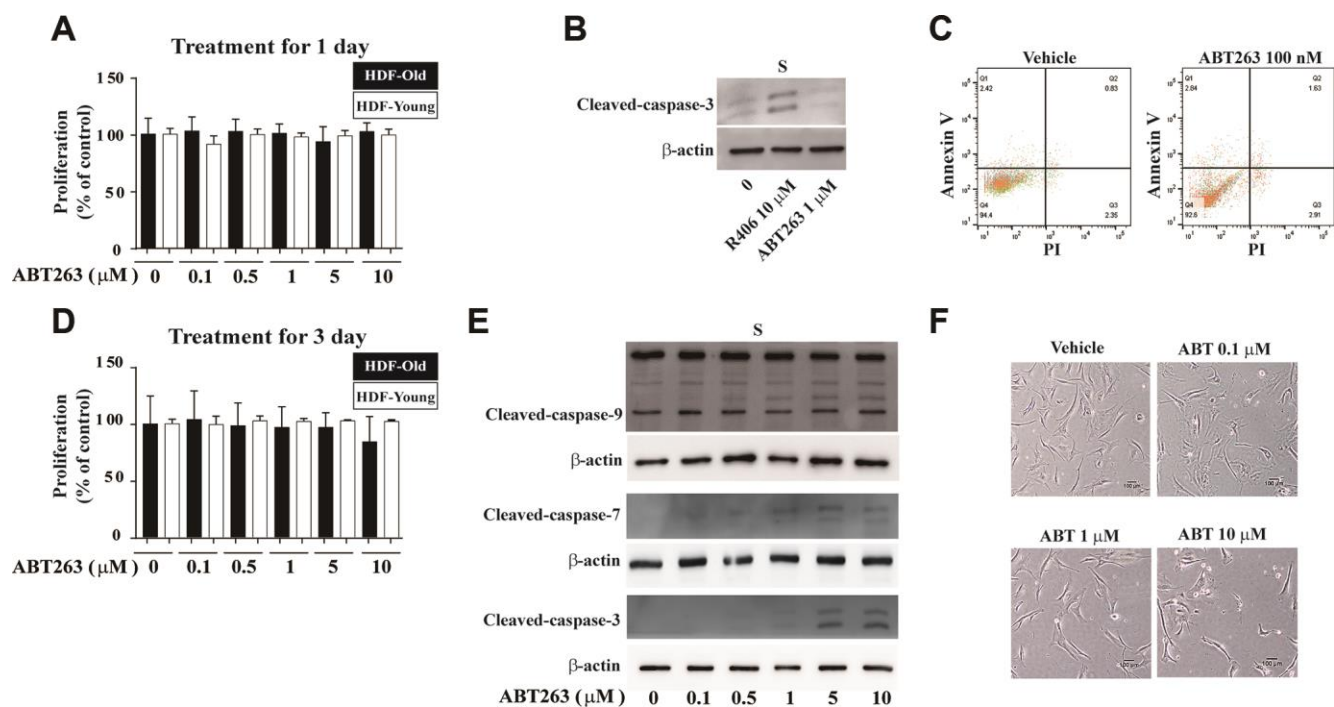
Supplementary Figure 4. ABT263 for one day treatment did not exhibit senolytic effect in the RS model. (**A**) Senescent HDFs (HDF-old) and non-senescent HDFs (HDF-young) were treated with DMSO or ABT263 (0.1, 0.5, 1, 5, 10 μM) for one day, and then CCK-1 assays were conducted to investigate cell viability. (**B**) Senescent HDFs were treated with DMSO or R406 (10 μM) or ABT263 100 nM for one day and then western blot assay (anti-caspase-3 antibody) was conducted. (**C**) Senescent HDF cell were treated with DMSO or ABT263 (100 nM) for one day and flow cytometry was conducted after Annexin V/PI staining. (**D**, **E**) HDF-old and HDF-young were treated with DMSO or ABT263 (0.1, 0.5, 1, 5, 10 μM) for three days. Then, (**D**) CCK-1 assays and (**E**) western blot assays (anti-caspase-9, anti-caspase-7, and anti-caspase-3 antibodies) were conducted. (**F**) Cell morphological change. Senescent HDFs were treated with DMSO or ABT263 (0.1, 1, 10 μM) for one day. Images were randomly captured by inverted microscopy (scale bar: 100 μm).
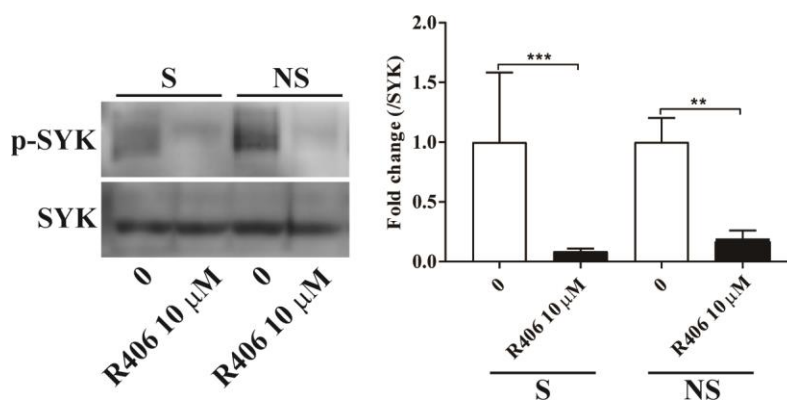
Supplementary Figure 5. R406 inhibited phosphorylation of SYK in both senescent and non-senescent HDFs. Senescent (S) and non-senescent (NS) HDFs were treated with DMSO or R406 (10 μM) for 1 h and then western blot assays with anti-SYK antibodies were conducted. *$p<0.05$, **$p<0.01$, ***$P<0.001$.

Supplementary Table

Supplementary Table 1. HTS results for selecting compounds that induce cytotoxicity or ROS levels in senescent HDFs.

Low proliferation			High ROS level		
Cell and drug conc.	HGPS 5 μM	HDF 0.5 μM	Cell and drug conc.	HGPS 5 μM	HDF 0.5 μM
Drug name	ROS level	Proliferation	Drug name	ROS level	Proliferation
OSI-027	0.94	0.686	Afatinib	2.25	0.838
Saracatinib	0.9	0.658	Dovitinib	2.48	0.908
SGI-1776 free base	1.24	0.657	Ponatinib	2.49	1.672
WYE-125132	1.16	0.653	CCT129202	3.64	1.267
PD184352	1.4	0.649	AZD5438	2.42	0.839
Bosutinib	1.66	0.648	IKK-16	2.37	0.886
Selumetinib	1.05	0.603	AZD3463	3.35	1.235
			GZD824	2.22	1.274
			BIO	2.38	0.882
Low proliferation and Low ROS level			**Low proliferation and High ROS level**		
Cell and drug conc.	HGPS 5 μM	HDF 0.5 μM	Cell and drug conc.	HGPS 5 μM	HDF 0.5 μM
Drug name	ROS level	Proliferation	Drug name	ROS level	Proliferation
LY2784544	0.88	0.678	Nintedanib	2.04	0.680
NVP-BHG712	0.75	0.677	Axitinib	2.1	0.619
R406 (Tamatinib)	0.81	0.645			

Supplementary Video

Please browse Full video version to see the data of Supplementary Video 1.

Supplementary Video 1. R406-induced morphological changes in senescent HDFs. Senescent HDFs were respectively treated with (**A**) DMSO, (**B**) R406 (10 μM), and (**C**) ABT263 (1 μM) and then time-laps imaging was conducted (Date: hours).